# Accepted Manuscript

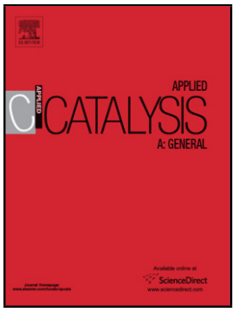

Title: Catalytic Cracking of n-Hexane for Producing Propylene on MCM-22 Zeolites

Author: Yong Wang Toshiyuki Yokoi Seitaro Namba Junko N. Kondo Takashi Tatsumi

PII: S0926-860X(14)00769-8
DOI: http://dx.doi.org/doi:10.1016/j.apcata.2014.12.018
Reference: APCATA 15156

To appear in: *Applied Catalysis A: General*

Received date: 14-9-2014
Revised date: 5-12-2014
Accepted date: 10-12-2014

Please cite this article as: Y. Wang, T. Yokoi, S. Namba, J.N. Kondo, T. Tatsumi, Catalytic Cracking of n-Hexane for Producing Propylene on MCM-22 Zeolites, *Applied Catalysis A, General* (2014), http://dx.doi.org/10.1016/j.apcata.2014.12.018

# Catalytic Cracking of n-Hexane for Producing Propylene on MCM-22 Zeolites

Yong Wang, Toshiyuki Yokoi*, Seitaro Namba, Junko N. Kondo, Takashi Tatsumi

*Chemical Resources Laboratory, Tokyo Institute of Technology, 4259 Nagatsuta, Midori-ku, Yokohama 226-8503, Japan*

**E-mail yokoi.t.ab@m.titech.ac.jp (T. Yokoi), Fax +81 45 924 5282*

## Abstract:

The catalytic cracking of n-hexane for producing propylene on MCM-22 catalysts was carried out as a model reaction of naphtha cracking. H-MCM-22 catalysts with different Si/Al ratios were prepared by direct or post-synthesis methods. The propylene selectivity was improved with an increase in the Si/Al ratio. Dealumination of H-MCM-22 with ammonium hexaflurosilicate (AHFS) (Del-Al-MCM-22) resulted in the increase in the catalytic life and propylene selectivity at a very high n-hexane conversion. This may be attributed to the decrease in the amount of Lewis acid sites which accelerate the hydride transfer and resultant coke formation. Del-Al-MCM-22 (Si/Al = 62) catalyst showed a high propylene selectivity (40 C-%) which was higher than H-ZSM-5 and H-Beta catalysts with similar Si/Al ratios at a high n-hexane conversion of 95%. Moreover, it showed a catalytic life comparable with H-ZSM-5 and longer than H-Beta catalyst.

*Keywords:* Catalytic cracking; Dealumination of H-MCM-22; Lewis acid site

## 1. Introduction

Light alkenes, in particular propylene, which are mainly supplied as a by-product of ethylene production through the thermal cracking of naphtha, are acquiring more and more significance in chemical industry. It is known that the thermal cracking is an energy intensive process, where the product distribution, especially the ratio of propylene to ethylene, is hard to control. Therefore, catalytic cracking of naphtha has been drawing increasing attention [1]. The catalytic cracking of alkanes over acidic zeolite catalysts gives a high propylene/ethylene ratio, since the transformation of long-chain alkanes to short-chain alkenes occurs at least partly via the carbenium ion/β-scission mechanism, i.e. the classical bimolecular cracking [2]. Compared with the thermal steam cracking, the catalytic cracking of naphtha which is carried out at lower temperatures would consume 20% less energy and reduce $CO_2$ emission by approximately 20% [1].

The catalytic cracking of light alkanes, such as pentane, hexane, heptane and octane, has been studied over various zeolite catalysts as a test reaction of naphtha cracking to clarify the performance of catalysts and the reaction mechanism [3]. There are many reports on cracking of alkanes at relatively low temperatures to allow discussion on the reaction mechanism and/or the effects of structure of zeolites [3-12]. However, there are only a few papers dealing with the catalysts working at high temperatures above 873 K which is necessary in order to obtain high alkene yields. Among the catalysts examined for the catalytic cracking, ZSM-5 zeolite has been recognized as a prime candidate because of its high thermal and hydrothermal stabilities and its considerable resistance to deactivation caused by coking as well as its strong acidity [1, 13-14]. Yoshimura et al. [1] have carried out the cracking of light naphtha in the presence of steam at 923 K and found that the addition of lanthanum (10 wt. %) to H-ZSM-5 (Si/Al = 100) enhanced the yield of ethylene and propylene up to 61 C-% and that the ethylene/propylene ratio in the product was approximately 0.7, which corresponds to a higher proportion of propylene than the composition obtained by using the current steam cracking. Moreover, further addition of phosphorus (2 wt. %) improved the stability. Recently, dealuminated MCM-68 catalyst with multidimensional channels of 10-MR and 12-MR has also been reported to exhibit a high propylene selectivity of 45 C-% [15]. However, the selectivity to propylene is uncertain when the conversion approaches 100%.

MCM-22, a kind of layered zeolite invented by Mobil in 1990 [16], belongs to the MWW type zeolite and possesses two independent pore systems. One consists of two-dimensional sinusoidal channels composed of slightly elliptical 10-MR, and the other is characteristic of 12-MR supercages accessible by 10-MR windows [17]. In addition, half supercages form surface pockets on the outer crystal surfaces. Because of its unique structure, MCM-22 zeolite has been proved to be a shape-selective catalyst in the alkylation [18, 19], disproportionation and isomerization [20-23], etc. Obviously, the acid properties (amount, location, type and strength) can also play important roles in these catalytic reactions. As we known, the acid properties are closely related to the Si/Al ratio in the zeolite.

A number of studies dealt with the synthesis of MCM-22 zeolite, concluding that only a very narrow range of the Si/Al ratio of about 10 – 25 is suitable for the synthesis of pure MCM-22 zeolite [24, 25]. Besides the direct synthesis methods, post-synthesis methods are also frequently used for preparing high silica zeolites. Post-synthesis of highly crystalline MWW zeolite with variable Si/Al ratios in a wide range (12 – 500) through the structural conversion of deboronated Si-MWW zeolite to lamellar Al-MWW zeolite precursor has been studied by Liu et al. [26]. They found that the amount and strength of Brønsted acid sites in H-MCM-22 zeolite both decreased with increasing Si/Al ratios. Another method for obtaining high silica MCM-22 zeolites is dealumination including acid leaching, hydrothermal treatment, combination of steaming and acid leaching, ammonium hexafluorosilicate (AHFS) treatment [20, 27-30], etc. Obviously, the acid properties in dealuminated MCM-22 are dependent on the different delamination methods.

MCM-22 has also proved to be a good cracking zeolite additive for FCC process [31, 32]. Corma et al. [32] found that when used as cracking additive, MCM-22 produced less total gases, as well as less dry gases, with a lower loss of gasoline than ZSM-5. Moreover, MCM-22 showed higher propylene/propane and butane/butane ratio and a good steam stability which was even higher than that of the ZSM-5 zeolite. The catalytic performance of MCM-22 in n-heptane cracking have been investigated by Meloni et al. [33], who found that a very fast initial deactivation was occurred, due to trapping of carbonaceous compounds (coke) in the large cages with small apertures. They suggested that n-heptane cracking occurs through the classical carbenium ion chain mechanism in the supercages, however it occurs through protolysis in the sinusoidal channels, the bimolecular reaction of hydride transfer being impossible in the narrow space available near the protonic sites. Though the role of shape selectivity on the catalytic performance was explained in the above paper, the role of acid properties including the acid amount, strength and type was seldom investigated.

In this study, the catalytic performance of MCM-22 catalysts with different Si/Al ratios synthesized and prepared by post-synthesis and treated with AHFS was investigated for the catalytic cracking of n-hexane as a model reaction of naphtha cracking to produce propylene. In addition, the relationship between the catalytic performance and the acid properties of the catalysts was discussed.

## 2. Experimental

### *2.1. Catalyst preparation*

H-MCM-22 zeolite catalysts with different Si/Al ratios were prepared by two methods according to literature [26, 34]. (1) Direct synthesis method was used for the synthesis of zeolites with high Al contents. The MCM-22 lamellar precursors were hydrothermally synthesized by using hexamethyleneimine (HMI) as a structure-directing agent (SDA). Fumed silica (Cab-o-sil M5) and sodium aluminate (58.3% $Al_2O_3$, 32.3% $Na_2O$) were used as Si and Al sources, respectively, and sodium hydroxide was used to adjust the gel pH. Deboronated MWW (Del-B-MWW) obtained by calcination of MWW borosilicate zeolite at 873 K for 20 h, followed by refluxing in 6 M $HNO_3$ at 393 K for 20 h, was used as seed to speed up the crystallization. The resulting mixture had a molar composition of 1 $SiO_2$ : 0.15 $Na_2O$ : (0.0125 - 0.025) $Al_2O_3$ : 0.9 HMI : 45 $H_2O$. (2) The MWW-type precursors with low Al contents were synthesized by a post-synthesis method. Del-B-MWW zeolite was used as a Si source and added into an aqueous solution of sodium aluminate and HMI under stirring. The resulting mixture had a molar composition of 1 $SiO_2$ : (0.005 - 0.007) $Al_2O_3$: 1 HMI: 30 $H_2O$. The crystallization was carried out in rotated (20 rpm) Teflon-lined stainless autoclaves under autogenous pressure at 423 K for 5 days. The samples were filtered, washed, and dried at 373 K to produce lamellar precursors with a wide range of Si/Al ratios. Direct calcination of the samples at 823 K for 10 h resulted in the products with the 3D MWW structure. The Na-form MCM-22 was transformed into the H-form by treating it with 1 M $NH_4NO_3$ twice at 353 K for 2 h, followed by calcination in air at 773 K for 2 h. The H-form MCM-22 zeolites prepared by direct and post-synthesis methods were named H-MCM-22 (n) and Post-H-MCM-22 (n), respectively, in which n denotes the Si/Al molar ratio determined by ICP-AES analysis.

Dealuminated MCM-22 (Del-Al-MCM-22) catalysts were obtained from H-MCM-22 (Si/Al = 19) by the dealumination with aqueous solution of ammonium hexaflurosilicate (AHFS) at 363 K for 3 h. The Del-Al-MCM-22 catalysts with different Al contents were obtained by varying the concentration of AHFS solution from 0.005 to 0.05 M. For control, a small-sized H-ZSM-5 catalyst with Si/Al = 66 was synthesized according to literature [13] and H-Beta catalyst with Si/Al = 67 was obtained from H-Beta (Si/Al = 12) (Reference Catalyst, The Catalysis Society of Japan) by dealumination with 1 M $HNO_3$ solution at 393 K for 1 h.

### *2.2. Catalyst characterizations*

The catalysts were characterized by various techniques. The Si/Al ratios were determined by inductively coupled plasma-atomic emission spectrometer (ICP-AES) on a Shimadzu ICPE-9000. The X-ray diffraction (XRD) patterns were recorded on a Rint-Ultima III (Rigaku) diffractometry using a Cu Kα X-ray source. The $N_2$ adsorption was carried out at 77 K on a Belsorp-mini II (BEL Japan) instrument. The crystal morphology and size were examined with a Hitachi S-5200 field-emission scanning electron microscope (FE-SEM). Thermogravimetric analyses (TGA) were carried out on a Mettler TGA/SDT apparatus in air atmosphere. Temperature-programmed desorption of ammonia ($NH_3$-TPD) spectra were recorded on a Multitrack TPD equipment (Japan BEL). IR spectra were collected on a Nicolet NEXUS-FTIR-670 spectrometer. The IR spectra of adsorbed pyridine were recorded as follows: a self-supported wafer (9.6 mg $cm^{-2}$ in thickness and 2 cm in diameter) was set in a quartz IR cell, sealed with $CaF_2$ windows, and then was evacuated at 723 K for 2 h before the pyridine adsorption. The adsorption was carried out by exposing the wafer to pyridine vapor (1.3 kPa) at 423 K for 0.5 h. The physisorbed pyridine was then removed by evacuation at 423 K for 1 h. The IR spectra were recorded at 423 K.

### *2.3. Catalytic cracking*

The catalytic cracking of n-hexane was carried out with a fixed-bed flow reactor under atmospheric pressure. Typically, 0.1 g of catalyst (18 – 30 mesh) was put into a tubular reactor (6 mm in i. d.) and activated in an air flow of 20 ml $min^{-1}$ at 923 K for 1 h. After the reactor temperature was adjusted to the desired, n-hexane (Wako Pure Chemicals Ind.) vapor diluted in helium was fed into the reactor. The initial partial pressure of n-hexane was set at 6 kPa. To investigate the effect of contact time, the ratio of the catalyst weight to the n-hexane flow rate ($W/F_{n\text{-hexane}}$) was varied from 1.6 to 64 g-cat h/mol-n-hexane by changing the catalyst amount.

The reaction products were analyzed with an on-line gas chromatograph (Shimadzu, GC-14B) with an FID detector and a HP-AL/S column (50 m × 0.32 mm × 8 μm). The selectivities to the products were calculated based on the carbon numbers. The coke amount was calculated by thermogravimetric analysis (TGA). The weight loss from 673 to 1073 K in each TG profile was defined as the contents of coke on the used catalyst.

## 3. Results and discussion

### *3.1. Physicochemical characteristics of the zeolites*

All of the H-MCM-22 zeolites synthesized in this study had the MWW topology and a relatively high crystallinity, and contained no impurity of other phase as detected by XRD patterns (Fig. 1A). As shown in Table 1, the H-MCM-22 samples had reasonably high BET surface areas in the range of 448 - 540 $m^2$ $g^{-1}$ as determined by $N_2$ adsorption, which indicated that they were of good quality. The images of scanning electron micrographs (SEM) revealed that both of H-MCM-22 (Si/Al = 19) and Post-H-MCM-22 (Si/Al = 100) samples were composed of flake-like crystals, approximately 500 nm in length and 50 nm in thickness (Fig. 2a and 2b). Thus, the crystal morphology and size were not dependent on the Si/Al ratio in the gels and the synthesis method. The Del-Al-MCM-22 samples with different Al contents were further characterized by powder XRD patterns (Fig. 1B). After dealumination by AHFS, little change was observed in their diffraction patterns compared with those of the parent material. Namely, the crystal structure of MCM-22 zeolite essentially remained.

Table 1 lists the Si/Al ratios and textural properties of Del-Al-MCM-22 zeolite catalysts. It can be seen that AHFS is an effective dealumination reagent for MCM-22 zeolite, and more than 40% of the aluminum atoms can be removed by the treatment with 0.005 M AHFS solution. With an increase in the AHFS concentration, the Si/Al ratio increased, which is consistent with the literature [30]. The specific surface area and micropore pore volume of of Del-Al-MCM-22 samples are also listed in Table 1. It can be seen that with an increase in the Si/Al ratio of the Del-Al-MCM-22 samples, viz. with an increasing in the AHFS concentration, the surface area and the micropore volume of the samples slightly decreased, while the external surface area was almost constant. On the other hand, the AHFS treatment, especially with high AHFS concentration, resulted in a significant fragmentation of crystal morphology to form a number of agglomerates (Fig. 2d). The formation of agglomerates could happen through binding of the surface hydroxyl groups (Si-OH) of neighboring crystallites, which can be facilitated in the presence of a chemical agent like AHFS [35].

Fig. 3 shows the $NH_3$-TPD profiles of H-MCM-22 and Del-Al-MCM-22 catalysts with different Al contents. As shown in Fig. 3, all these profiles were composed of two desorption peaks so-called *l*-peak and *h*-peak. The *l*-peak corresponds to $NH_3$ adsorbed on non-acidic –OH groups and on $NH_4^+$ by hydrogen bonding, while the *h*-peak corresponds to $NH_3$ adsorbed on true acid sites [36, 37]. Thus, the acid amount was calculated by the area of *h*-peak. The acid amount corresponded to only 63-77% of the total Al content in H-MCM-22 zeolites (Table 1). The low concentration of acid relative to that of Al are attributed to the fact that the portion of Al incorporated into the MCM-22 framework was not very high, regardless of the direct or post synthesis methods. Obviously, the acid amount was decreased with the Si/Al ratio increased (Fig. 3A, Table 1). On the other hand, the acid amount was gradually decreased with an increase in the AHFS concentration (Fig. 3B, Table 1), which means the AHFS treatment is an effective dealumination method for MCM-22 zeolite.

H-ZSM-5 and H-Beta catalysts had relatively high crystallinities as indicated by XRD patterns (not shown) and reasonably high BET surface areas (Table 1). As shown in Fig. 2, H-ZSM-5 (Si/Al = 66) and H-Beta (Si/Al = 67) were composed of coffin-like crystals with an average size of about 200 nm and sphere-like crystals with an average size of about 100 nm, respectively (Figs. 2e and 2f). In addition, the Si/Al ratio and acid amount of H-ZSM-5 and H-Beta catalysts were similar to those of Del-Al-MCM-22 catalyst (Table 1).

### *3.2. Catalytic cracking of n-hexane over H-MCM-22 catalysts*

#### *3.2.1. Effect of reaction temperature*

The effect of the reaction temperature on the catalytic cracking of n-hexane over H-MCM-22 (Si/Al = 19) is shown in Fig. 4. The initial conversion of n-hexane increased with an increase in the temperature, achieving nearly 100% at 923 K. The selectivity to propylene was almost constant in the temperature ranging between 723 and 923 K. With an increase in the reaction temperature, apparently butenes once formed were gradually transformed into aromatic compounds, resulting in the decrease in the selectivity to butenes accompanied with the increase in the selectivity to BTX (benzene, toluene, and xylenes). The selectivity to ethylene was low compared with those to other alkenes at low temperature; however, the value increased steeply with an increase in the reaction temperature. Ethylene is formed via primary carbenium ions, regardless of whether the monomolecular mechanism or the bimolecular mechanism operates [5, 7] and therefore the apparent activation energy for ethylene formation should be high. Thus, the higher reaction temperature is of benefit to the higher ethylene yield. Moreover, the cracking via the monomolecular mechanism may be of more advantage in the ethylene formation. The selectivities to propane and butanes decreased with an increase in the reaction temperature, because the subsequent reactions of propane and butanes take place at high temperatures, resulting in the formation of alkenes, BTX and so on [38]. In addition, the selectivities to methane and ethane, which form solely via the monomolecular mechanism, are higher at the higher reaction temperatures. These findings clearly indicate that the cracking via the monomolecular mechanism is more predominant at the high temperature.

According to the product distributions at different reaction temperatures, we conclude that higher reaction temperature is beneficial to n-hexane conversion and propylene production. Kubo et al. reported similar results in n-heptane cracking over H-ZSM-5 [14].

### *3.2.2. Effect of contact time*

The effect of the contact time on the reaction was investigated. The contact time expressed as the ratio of the catalyst weight to the n-hexane flow rate ($W/F_{\text{n-hexane}}$) was changed by the change of catalyst weight to keep the contribution of the thermal cracking constant. As shown in Fig. 5, the conversion of n-hexane increased with an increase in $W/F_{\text{n-hexane}}$, achieving nearly 100% at the $W/F_{\text{n-hexane}}$ of 64 g-cat h/mol-n-hexane. Fig. 5 indicates that the decrease in the selectivities to propylene and butenes is accompanied with the increase in the selectivity to BTX, suggesting that BTX is formed mainly from propylene and butenes. On the other hand, primary carbenium ions would be relatively easy to produce at the high reaction temperature of 923 K [5, 7]. Therefore, ethylene would be formed not only by n-hexane cracking but also by butanes and/or propane cracking, resulting in an increase in the ethylene selectivity [38]. Meanwhile, the selectivities to propane and butanes decreased with an increase in the conversion, while those to methane and ethane simultaneously increased.

### *3.2.3. Effect of Al content*

It is widely known that acidity of zeolites is largely dependent on their Si/Al molar ratios. In order to elucidate the effect of the acidity on the catalytic cracking of n-hexane, H-MCM-22 zeolites with different Si/Al ratios were employed as catalysts. First, effect of the Al content on catalytic activity was investigated. We consider that n-hexane cracking at such high temperatures is the sum of the catalytic cracking and the thermal cracking since the contribution of thermal cracking is not negligible. If both the catalytic cracking and the thermal cracking at high temperatures obey the first-order kinetics, the following equation is derived;

$$k_c \, W/F = \ln(1/1\text{-}x) - \ln(1/1\text{-}x_p). \qquad \text{eq. (1)}$$

where $k_c$ is the rate constant for the catalytic cracking, x and $x_p$ are the conversion for the n-hexane cracking with and without catalyst, respectively [14]. Fig. 6 shows the dependence of $k_c$ on the acid amount of H-MCM-22 catalysts at different reaction temperatures. The linear relationship between log $k_c$ and log acid amount of H-MCM-22 catalyst was observed at every reaction temperature. As shown in Fig. 6, the slopes of the straight line observed in the log $k_c$ vs. log (Acid amount) plots are 1.8, 1.6, and 1.3 at 823, 873, and 923 K, respectively. The $k_c$ is almost proportional to the acid site density at 923 K; however, at lower temperatures the effect of the acid site density is enhanced with a decrease in reaction temperature. Haag et al. reported that the catalytic activity in the catalytic cracking of n-hexane at 811 K over H-ZSM-5 is proportional to the acid site density [39-41]. A similar dependence of n-hexane and n-heptane cracking on the acid density over H-ZSM-5 with various Si/Al ratios has been reported by Post et al. and Kubo et al. [6, 14].

Then, the effect of the Al content on products distribution was investigated. Fig. 7 shows the relationship between the selectivities and the acid amount of H-MCM-22 catalysts at an n-hexane conversion of ca. 80%. It can be seen that, with a decrease in the acid amount, propylene and butenes selectivities slightly increased while ethylene and BTX selectivities slightly decreased. These findings suggest that the decrease in the acid amount suppressed the secondary reactions (hydride transfer and cyclization-aromatization) of propylene and butenes to form BTX. Thus the H-MCM-22 catalysts with the higher Si/Al ratios showed the higher propylene selectivity in the catalytic cracking of n-hexane. Meanwhile, the subsequent cracking reaction of butanes and/or propane to form ethylene at high reaction temperature of 923 K was reduced with a decrease in the acid amount, resulting in the decrease in the ethylene selectivity accompanied with the increase in the selectivties to butanes and propane (not shown here).

Besides activity and selectivity, stability is another important factor for applications of catalysts in industry. Fig. 8 shows the change in n-hexane conversion with time on stream (TOS) for H-MCM-22 catalysts with different Si/Al ratios. Obviously, the initial activity and deactivation rate closely depended on the Si/Al ratio. The H-MCM-22 catalyst with higher Al contents (Si/Al = 19 and 34) gave nearly 100% n-hexane conversion at the initial stage, whereas the catalyst with a lower Al content (Si/Al = 100) showed only ca. 80% conversion of n-hexane. A sharp decrease in the n-hexane conversion with TOS was observed for the H-MCM-22 catalyst with high Al contents. For example, the n-hexane conversion of H-MCM-22 (Si/Al = 19) decreased to ca. 60% at TOS of 210 min. This deactivation was probably due to the deposition of a large amount of coke (95 mg/g-catalyst). The formation of large amount of coke can be explained by two possible reasons. One reason may be related to the high amount of acid sites, which would accelerate the secondary reactions including hydride transfer, cyclization-aromatization and dehydrogenating coupling, etc. and resultant coke formation. Another reason may be related to the special structure of MCM-22 zeolite. The nonconnected property between 12- and 10-MR channels and the 10-MR window openings accessible to the 12-MR supercages would increase the diffusion limitation, leading to the high coke formation. The coke composition and the mode of deactivation in n-heptane cracking over MCM-22 zeolite had been investigated and established by Meloni et al. [33]. In the case of Post-H-MCM-22 (Si/Al = 100) catalyst, the deactivation rate was relative slow, due to the smaller amount of acid sites leading to the suppression of hydride transfer and coke formation (14 mg/g-catalyst). These results indicate that H-MCM-22 catalysts with lower Al contents exhibit a better stability than the catalyst with higher Al contents.

In addition, the crystallite size strongly might affect the catalytic stability. Mochizuki et al. reported the small-sized H-ZSM-5 catalyst exhibits a higher stability in n-hexane catalytic cracking, owing to large external surface area and short diffusion path length [13]. However, in our present study, MCM-22 catalysts with different Al contents by direct or post-synthesis method had similar crystallite morphology and sizes (Fig 2a – 2d). Thus, the influence of crystallite size on catalytic stability could not be examined.

### *3.3. Catalytic cracking of n-hexane over Del-Al-MCM-22 catalysts*

From the results reported above, H-MCM-22 catalysts with lower Al contents prepared from the post-synthesis method exhibited the higher propylene selectivity. However, the catalytic stability was still not satisfactory. Thus, the catalytic performance of several high-silica MCM-22 zeolites prepared by the dealumination was further investigated.

Fig. 9 shows the change in n-hexane conversion with TOS for H-MCM-22 (Si/Al = 19) and Del-Al-MCM-22 catalysts with different Si/Al ratios. The stability of Del-Al-MCM-22 catalysts was greatly improved by the dealumination, though the initial n-hexane conversion slightly decreased. In the case of Del-Al-MCM-22 (Si/Al = 62), the initial n-hexane conversion was about 95%, and only slightly decreased to 88% at 210 min. This also may be due to the smaller amount of acid sites in the Del-Al-MCM-22 catalyst, resulting in suppression of the hydride transfer and coke formation (22 mg/g-catalyst). It is noted that the catalytic stabilities of Post-H-MCM-22 (Si/Al = 66) and Del-Al-MCM-22 (Si/Al = 62) catalysts was different, though they had similar Si/Al ratios and acid amounts. This finding indicates that some other factor than the acid amount affects the catalytic stability, which is to be discussed in Section 3.5. In addition, the amount of coke on the Post-H-MCM-22 (Si/Al = 66) and Del-Al-MCM-22 (Si/Al = 62) catalysts was nearly the same, however the stabilities was different, indicating the different coke composition and location on the two catalysts. This may be due to the difference in the type, strength and location of acid sites.

Fig. 10 shows the changes in selectivities to alkenes and BTX in the n-hexane conversion on H-MCM-22 (Si/Al = 19) and Del-Al-MCM-22 catalysts with different Si/Al ratios. As shown in Fig. 10, for H-MCM-22 (Si/Al = 19) catalyst, the selectivities to propylene and butenes were decreased along with increasing n-hexane conversion, while those to ethylene and BTX were increased. The selectivity to propylene was decreased from 41 to 30 C-% when the n-hexane conversion was increased from 60% to nearly 100%. Compared with the parent H-MCM-22(Si/Al = 19) catalyst, Del-Al-MCM-22 catalysts showed high selectivities to propylene and butenes and simultaneously low selectivities to ethylene and BTX at high n-hexane conversions. In addition, Del-Al-MCM-22 catalysts showed higher selectivities to butanes and propane at high n-hexane conversions (not shown here). For example, in the case of Del-Al-MCM-22(Si/Al = 62), the propylene selectivity was kept almost constant (*ca*. 40 C-%) even at a high n-hexane conversion of 95%. These findings indicate that the secondary reactions to form BTX from propylene and butenes and the cracking reaction of butanes and/or propane to form ethylene at high reaction temperature of 923 K were suppressed when the acid amount of catalyst was decreased.

### *3.4. Comparison of the catalytic performance of Del-Al-MCM-22 with H-ZSM-5 and H-Beta catalysts*

In the present study, the catalytic performance of Del-Al-MCM-22 was also compared with that of H-ZSM-5 and H-Beta catalysts, which are the catalyst mostly used in FCC process [31, 32]. Fig. 11 shows the change in n-hexane conversion with TOS for H-ZSM-5, H-Beta and Del-Al-MCM-22 catalysts with similar Si/Al ratios and acid amounts. Among these catalysts investigated, the H-ZSM-5 (Si/Al = 66) catalyst gave a high initial n-hexane conversion of nearly 100% and the highest stability. The amount of coke formed during the reaction for 210 min was very low (29 mg/g-catalyst). This may be related to the tridirectional 10-MR channels in ZSM-5 zeolite, which is beneficial to the mass transfer, leading to very low deactivation. The Del-Al-MCM-22 (Si/Al = 62) catalyst showed a little lower initial n-hexane conversion (95%); however the stability was still good. The resistivity of Del-Al-MCM-22 (22 mg/g-catalyst) to coke formation was as high as that of H-ZSM-5, probably due to its acid strength and density of acid sites are similar to those of H-ZSM-5 [36]. Although H-Beta (Si/Al = 67) catalyst showed a high initial n-hexane conversion (nearly 100%), the amount of coke formed thereon during the reaction for 210 min (107 mg/g-catalyst) was much higher than those on the other two catalysts, leading to a significant deactivation. Despite the milder acidity of H-Beta catalyst compared with H-MCM-22 and H-ZSM-5 catalysts [42], the polymerization of olefins and the successive formation of coke components in the 3-dimensional 12-MR micropores and their wide intersections may predominantly occur [15]. A similar result has been reported by Corma et al., who suggest that the stability of H-MCM-22 zeolite is intermediate between those of H-Beta and H-ZSM-5 in n-heptane cracking at the lower temperature of 723 K， mainly because MCM-22 zeolite has larger pores and/or cavities than ZSM-5 and smaller ones than Beta zeolite [31]. In addition, the crystallite size and morphology of zeolite also have influenced on the mass transfer. The flake-like crystal of MCM-22 zeolite is beneficial to the mass transfer, compared to the coffin-like crystal

ZSM-5 and sphere-like crystal Beta zeolite (Fig. 2).

Fig. 12 shows the changes in selectivities to alkenes and BTX with n-hexane conversion on H-ZSM-5, H-Beta and Del-Al-MCM-22 catalysts. As shown in Fig. 12, for H-ZSM-5 and H-Beta catalyst, the selectivities to propylene and butenes steeply decreased with an increase in n-hexane conversion, while those to ethylene and BTX increased drastically. However, in the case of Del-Al-MCM-22 (Si/Al = 62) catalyst, the propylene selectivity was kept almost constant (*ca*. 40 C-%), even at an n-hexane conversion as high as 95%. Moreover, when the n-hexane conversion was higher than 95%, it showed a lower BTX selectivity than either H-ZSM-5 or H-Beta catalysts, which could be due to the inferior hydride transfer ability of MCM-22 catalyst at high n-hexane conversions [43]. These findings indicate that the catalytic performance of Del-Al-MCM-22 catalyst is superior to that of H-ZSM-5 and H-Beta catalysts in the catalytic cracking of n-hexane to produce propylene under these reaction conditions.

### *3.5 Investigation of the relationship between catalytic performance and acidity of MCM-22 catalysts*

As shown in Figs. 6-10, the catalytic performance depended closely on the Si/Al ratio of H-MCM-22 and Del-Al-MCM-22 catalysts. With increasing Si/Al ratio of H-MCM-22 or Del-Al-MCM-22 catalysts, the acid amount was decreased (Fig. 3, Table 1), resulting in the decrease in the cracking activity of catalysts. H-MCM-22 catalysts with the higher Si/Al ratios and Del-Al-MCM-22 catalysts showed a higher propylene selectivity and longer catalytic life than H-MCM-22 catalysts with high Al contents. This could be ascribed to the decrease in the acid amount, which suppressed the secondary reaction of propylene and butenes and the hydride transfer to form coke. Similarly, Zhu et al. also reported the ZSM-5 zeolites with lower acid amount (higher Si/Al ratio) exhibited better performance in butene catalytic cracking to propylene and ethylene [44].

It is well know that not only the acid amount but also the acid strength and type of acid site, Brønsted or Lewis acid site affect the catalytic performance. However, the results of $NH_3$-TPD only showed the change of the acid amount. So, the pyridine-IR spectroscopy was investigated to provide more detailed information on the type and amount of acid sites and their strength.

Fig. 13 shows the IR spectra of H-MCM-22 catalysts with different Si/Al ratios before (A) and after (B) pyridine was absorbed and desorbed at 423 K. As shown in Fig. 13A, in the region of hydroxyl stretching vibration, the H-MCM-22 (Si/Al = 19) catalyst exhibited two strong bands at 3743 and 3615 $cm^{-1}$, which are attributed to external silanols and structural Si(Al)OH hydroxyls, respectively. In addition, two weak bands appeared at 3727 and 3663 $cm^{-1}$, which are assigned to internal silanols and hydroxyls related to extra-framework Al, respectively [20, 34]. The 3615 $cm^{-1}$ band gradually decreased in intensity with a decrease in Al content, indicating a decrease in the amount of Brønsted acid sites. In the case of Post-H-MCM-22 catalysts, the 3727 $cm^{-1}$ band increased significantly in intensity and a broad band around 3500 $cm^{-1}$ attributed to hydrogen bonded silanols appeared when the Al content was decreased. These facts indicate that Post-H-MCM-22 catalysts have more defect sites than the catalysts prepared by the direct synthesis method.

Then, the IR spectra of adsorbed pyridine in the range of pyridine ring-stretching modes after desorption at 423 K was measured, as shown in Fig. 13B. The bands at 1543 and 1454 cm$^{-1}$ were attributed to Brønsted acid sites (BAS) and Lewis acid sites (LAS), respectively. With a decrease in Al content, the intensity of the 1543 and 1454 cm$^{-1}$ band decreased simultaneously, indicating not only Brønsted acid but also Lewis acid decreased in amount. However, the ratio of BAS/LAS, which was calculated by using the area of peaks ascribed to the Brønsted and Lewis acid sites, for Post-H-MCM-22 catalysts was lower than that for H-MCM-22 catalysts; *e.g.*, the BAS/LAS ratios for Post-H-MCM-22 (Si/Al = 100) and H-MCM-22 (Si/Al = 19) were calculated to be 1.9 and 2.6, respectively. Thus, the Post-H-MCM-22 catalysts have higher proportion of Lewis acid sites than the H-MCM-22 catalysts prepared by the direct synthesis method. Based on the catalytic performance results shown in Figs. 8 and 9, Section 3.2.3, although the Post-H-MCM-22 catalysts exhibited better stabilities than the direct synthesized H-MCM-22 catalysts, their stabilities were not so high compared to the dealuminated MCM-22 catalysts. The possible reason may be due to the higher proportion of Lewis acid sites in the post synthesized MCM-22 zeolites. Since the Lewis acid sites interact with olefins to enhance their oligomerization and subsequent hydride transfer reactions, leading to the formation of coke products [45].

Similarly, Fig.14 shows the IR spectra of Del-Al-MCM-22 catalysts with different Si/Al ratios before (A) and after (B) pyridine was absorbed and desorbed at 423 K. The 3615 cm$^{-1}$ band gradually decreased in intensity; however the 3743 cm$^{-1}$ band increased with a progress of dealumination (Fig. 14A). Fig. 14B showed that the intensity of the 1543 and 1454 cm$^{-1}$ bands ascribed to Brønsted and Lewis acid sites, respectively, decreased with a progress of dealumination. These findings imply that aluminum atoms not only in the framework but also of extra-framework are removed by the AHFS treatment. Moreover the BAS/LAS ratio increased after the dealumination, which means that the Lewis acid sites are removed more readily than the Brønsted acid sites. Thus, it was deduced not only the acid amount but also the acid type was changed with dealumination using AHFS treatment. The BAS/LAS ratios for dealuminated MCM-22 catalysts were higher than that for H-MCM-22 (Si/Al = 19) catalyst; *e.g.*, the BAS/LAS ratios for Del-Al-MCM-22 (Si/Al = 62) and H-MCM-22 (Si/Al = 19) were calculated to be 4.3 and 2.6, respectively. Thus, the Del-Al-MCM-22 catalysts have lower proportion of Lewis acid sites than the parent H-MCM-22 catalyst. The superiority of Del-Al-MCM-22 catalysts in the catalytic life and propylene selectivity could be due to their smaller amount of Lewis acid sites which accelerate the hydride transfer and coke formation.

The distribution of the acid strength of Brønsted and Lewis acid sites can be measured from the thermal desorption of pyridine [46]. Fig. 15 shows the IR spectra in the pyridine vibration region of H-MCM-22 (Si/Al = 19) (A), Post-H-MCM-22 (Si/Al = 66) (B) and Del-Al-MCM-22 (Si/Al = 62) (C) catalysts after pyridine adsorption and following desorption at different temperatures. It is apparent that for all the catalysts, the intensity of the band ascribed to Brønsted acid sites decreased with desorption temperature increasing from 423 K to 723 K. For H-MCM-22 and Post-H-MCM-22 catalysts, the intensity of the band ascribed to Brønsted acid sites was reduced by ca. 75% and 90%, respectively when the temperature of desorption increased from 423 K to 723 K. No band was observed in the case of Del-Al-MCM-22 catalyst when the desorption temperature was increased to 723 K. These facts demonstrate that the Brønsted acid strength of Del-Al-MCM-22 catalyst is relatively low compared with that of parent H-MCM-22 and Post-H-MCM-22 catalysts. On the other hand, for H-MCM-22 and Del-Al-

MCM-22 catalysts, the intensity of band ascribed to Lewis acid sites also decreased with desorption temperature increased. When the desorption temperature was increased from 423 K to 723 K, the intensity of the band ascribed to Lewis acid sites was reduced by ca. 10% and 50% respectively, which suggests that the strength of Lewis acid is higher than that of Brønsted acid in these two catalysts. It is noted that the intensity of the band ascribed to Lewis acid sites was almost unchanged with desorption temperature increased in the case of Post-H-MCM-22 (Si/Al = 66), indicating that the strength of Lewis acid sites on Post-H-MCM-22 is higher than that of H-MCM-22 and Del-Al-MCM-22 catalysts. This could be a possible reason for the lower stability of Post-H-MCM-22 compared with Del-Al-MCM-22 catalyst in n-hexane cracking. According to the above findings, it is also concluded that the decrease in the strength of acid sites would be another reason for the higher propylene selectivity and stability of Del-Al-MCM-22 catalysts, since strong acid sites play a significant role in coke formation and coke formed on strong acid sites is much heavier than that formed on weak acid sites [47].

## 4. Conclusions

H-MCM-22 catalysts with higher Si/Al ratios prepared by the post-synthesis method showed higher propylene selectivity in catalytic cracking of n-hexane. This could be attributed to the smaller acid amount, which resulted in suppression of the secondary reaction of propylene and butenes. However, the catalytic stability was still not satisfactory. This can be explained by the fact that the Post-H-MCM-22 catalysts had more strong Lewis acid sites, which accelerate the hydride transfer and coke formation. The catalytic life and propylene selectivity at high n-hexane conversions were improved by dealumination using AHFS. This could be due to the smaller amount of Lewis acid sites and the decrease in the strength of acid sites. Del-Al-MCM-22 (Si/Al = 62) showed a higher propylene selectivity (40 C-%) than H-ZSM-5 (Si/Al = 66) and H-Beta (Si/Al = 67) catalysts with similar Si/Al ratios at a high n-hexane conversion of 95%. Moreover, the catalyst stability was comparable to that of H-ZSM-5 and higher than that of H-Beta catalyst.

Acknowledgements

This work was partially supported by the green sustainable chemistry project of New Energy and Industrial Technology Development Organization (NEDO).

## References

[1] Y. Yoshimura, N. Kijima, T. Hayakawa, K. Murata, K. Suzuki, F. Mizukami, K. Matano, T. Konishi, T. Oikawa, M. Saito, T. Shiojima, K. Shiozawa, K. Wakui, G. Sawada, K. Sato, S. Matsuo, N. Yamaoka, Catal. Surv. Jpn. 4 (2000) 157-167.

[2] W.O. Haag, R.M. Lago, P.B. Weisz, Faraday Discuss. Chem. Soc. 72 (1981) 317-330.

[3] K.A. Cumming, B.W. Wojciechowski, Catal. Rev. Sci. Eng. 38 (1996) 101-157

[4] W.O. Haag, R.M. Dessau, in: Proc. Proceedings of the Eighth International Congress on Catalysis, Berlin, vol. 2, 1984, 305-316.

[5] W.O. Haag, R.M. Dessau, R.M. Lago, Stud. Surf. Sci. Catal. 60 (1991) 255-265.

[6] A.F.H. Wielers, M. Waarkamp, M.F.M. Post, J. Catal. 127 (1991) 51–66.

[7] H. Krannila, W.O. Haag, B.C. Gates, J. Catal. 135 (1992) 115-124.

[8] S. Jolly, J. Saussey, M.M. Bettahar, J.C. Lavalley, E. Benazzi, Appl. Catal. A 156

(1997) 71-96.

[9] S.M. Babitz, B.A. Williams, J.T. Miller, R.Q. Snurr, W.O. Haag, H.H. Kung, Appl. Catal. A 179 (1999) 71-86.

[10] S. Kotrel, M.P. Rosynek, J.H. Lunsford, J. Catal. 191 (2000) 55-61.

[11] A. Corma, A.V. Orchille´s, Micropor. Mesopor. Mater. 35-36 (2000) 21-31.

[12] B.C. Gates, J.R. Katzer and G.C.A. Schuit, Chemistry of Catalytic Processes, McGraw-Hill, New York, 1979.

[13] H. Mochizuki, T. Yokoi, H. Imai, R. Watanabe, S. Namba, J.N. Kondo, T. Tatsumi, Micropor. Mesopor. Mater. 145 (2011) 165-171.

[14] K. Kubo, H. Iida, S. Namber, A. Igarashi, Micropor. Mesopor. Mater. 149 (2012) 126-133.

[15] S. Inagaki, K. Takechi, Y. Kubota, Chem. Commun. 46 (2010) 2662-2664.

[16] M.K. Rubin, P. Chu, US Patent 4954325, 1990.

[17] M.E. Leonowicz, J.A. Lawton, S.L. Lawton, M.K. Rubin, Science 264 (1994) 1910-1913.

[18] A. Corma, V. Martínez-Soria, E. Schnoeveld, J. Catal. 192 (2000) 163-173.

[19] B. Xue, J. Chen, N. Liu, J. Guo, J. Xu, C.F. Xu, Q.M. Shen, Y.X. Li, Catal. Comm. 56 (2014) 174-178.

[20] P. Wu, T. Komatsu, T. Yashima, Micropor. Mesopor. Mater. 22 (1998) 343-356.

[21] Y.J. Ji, B. Zhang, L. Xu, H.H. Wu, H.G. Peng, L. Chen, Y.M. Liu, P. Wu, J. Catal. 283(2011) 168-177.

[22] M. A. Asensi, A. Corma, A. Martínez, J. Catal. 158 (1996) 561-569.

[23] M.R. Mihályi, M. Kollár, S. Klébert, V. Mavrodinova, Appl. Catal. A 476 (2014)

19-25.

[24] A. Corma, C. Corell, J. Perezpariente, Zeolites 15 (1995) 2-8.

[25] M.J. Cheng, D.L. Tan, X.M. Liu, X.W. Han, X.H. Bao, L.W. Lin, Micropor. Mesopor. Mater. 42 (2001) 307-316.

[26] L. Liu, M. Cheng, D. Ma, G. Hu, X. Pan, X. Bao, Micropor. Mesopor. Mater. 94 (2006) 304-312.

[27] P. Matias, J.M. Lopes, P. Ayrault, S. Laforge, P. Magnoux, M. Guisnet, F. Ramoˆa Ribeiro, Appl. Catal. A 365 (2009) 207-213.

[28] P. Me´riaudeau, Vu A. Tuan, Vu T. Nghiem, F. Lefevbre, Vu T. Ha, J. Catal. 185 (1999) 378-385.

[29] R.M. Mihályi, M. Kollár, P. Király, Z. Karoly, V. Mavrodinova, Appl. Catal. A 417-418 (2012) 76-86.

[30] X.X. Zhu, S.L. Liu, Y.Q. Song, L.Y. Xu, Catal. Comm. 6 (2005) 742-746.

[31] A. Corma, V. GonzBlez-Alfaro, A.V. Orchillks, Appl. Catal. A 129 (1995) 203-215.

[32] A. Corma, J. Martinez-Triguero, J. Catal. 165 (1997) 102-120.

[33] D. Meloni, D. Martin, M. Guisnet, Appl. Catal. A 215 (2001) 67-79.

[34] A. Corma, C. Corell, J. Pérez-Pariente, J.M. Guil, R. Guil-López, S. Nicolopoulos, J. Gonzalez Calbet, M. Vallet-Regi, Zeolites 16 (1996) 7-14.

[35] C.S. Triantafillidis, A.G. Vlessidis, N.P. Evmiridis, Ing. Eng. Chem. Res. 39 (2000) 307-319.

[36] M. Niwa, M. Sawa, N. Katada, Y. Murakami, J. Phys. Chem. 99 (1995) 8812-8816.

[37] N. Katada, H. Igi, J. H. Kim, M. Niwa, J. Phys. Chem. B 101(1997) 5969-5977.

[38] G. Y. Jiang, L. Zhang, Z. Zhao, X. Y. Zhou, A.J. Duan, C.M. Xu, J.S. Gao, Appl.

Catal. A 340 (2008) 176-182.

[39] D.H. Olson, W.O. Haag, R.M. Lago, J. Catal. 61 (1980) 390-396.

[40] W.O. Haag, R.M. Lago, P.B. Weisz, Nature 309 (1984) 589-591.

[41] W.O. Haag, Stud. Surf. Sci. Catal. 84 (1994) 1375-1394.

[42] N. Katada, K. Suzuki, T. Noda, W. Miyatani, F. Taniguchi, M. Niwa, Appl. Catal. A 373 (2010) 208-213.

[43] A. K. Talukdar, K. G. Bhattacharyya, T. Baba, Y. Ono, Appl. Catal. A 213 (2001) 239-245.

[44] X.X. Zhu, S.L. Liu, Y.Q. Song, L.Y. Xu, Appl. Catal. A 288 (2005) 134-142.

[45] J. Čejka, B. Wichterlová, Catal. Rev. -Sci. Eng., 44 (2002) 375-421.

[46] P. Wu, T. Komatsu, T. Yashima, J. Phys. Chem. 99 (1995) 10923-10931.

[47] B. Wang, G. Manos, Ind. Eng. Chem. Res. 47 (2008) 2948-2955.

**Figure captions**

Fig. 1 XRD patterns of H-MCM-22 samples (A) with Si/Al ration of 19 (a), 34 (b), 66 (c) and 100 (d) and Del-Al-MCM-22 samples (B) with Si/Al ratio of 34 (b), 56 (c) and 62 (d).

Fig. 2 SEM images of H-MCM-22(Si/Al = 19) (a), Post-H-MCM-22(Si/Al = 100) (b), Del-Al-MCM-22(Si/Al = 34) (c), Del-Al-MCM-22(Si/Al = 62) (d), H-ZSM-5(Si/Al = 66) (e) and H-Beta(Si/Al = 67) (f) samples.

Fig. 3 $NH_3$-TPD profiles of H-MCM-22 (A) and Del-Al-MCM-22 (B) samples with different Si/Al ratios.

Fig. 4 Effect of reaction temperature on the catalytic cracking of n-hexane on H-MCM-22(Si/Al = 19). Reaction conditions: Cat., 0.1 g; $P_{\text{n-hexane}}$ = 6 kPa; $W/F_{\text{n-hexane}}$ = 64 g-cat h/mol-n-hexane; temp., 723 - 923 K, TOS = 15 min.

Fig. 5 Effect of contact time on the catalytic cracking of n-hexane on H-MCM-22(Si/Al = 19). Reaction conditions: $W/F_{\text{n-hexane}}$ = 6.4 - 64 g-cat h/mol-n-hexane; temp., 923 K, others see Fig. 4.

Fig. 6 Dependence of $k_c$ on the acid amount of H-MCM-22 catalysts at different reaction temperatures of 723 K (a), 823 K (b) and 923 K (c).

Fig. 7 Relationship between product selectivities and acid amount of H-MCM-22 catalysts at an n-hexane conversion of ca. 80%. Reaction conditions: $P_{\text{n-hexane}}$ = 6 kPa; temp., 923 K, TOS = 15 min.

Fig. 8 Change in n-hexane conversion with time on stream (TOS) for H-MCM-22 catalysts with different Si/Al ratios. Reaction conditions: temp., 923 K, others see Fig. 4.

Fig. 9 Change in n-hexane conversion with time on stream (TOS) for H-MCM-22(Si/Al = 19) and Del-Al-MCM-22 catalysts with different Si/Al ratio. Reaction conditions: temp., 923 K, others see Fig. 4.

Fig. 10 Changes in selectivities to $C_3^=$ (A), $C_2^=$ (B), $C_4^=$ (C) and BTX (D) with n-hexane conversion on H-MCM-22(Si/Al = 19) and Del-Al-MCM-22 catalysts with different Si/Al ratios. Reaction conditions: see Fig. 5.

Fig. 11 Change in n-hexane conversion with time on stream (TOS) for H-ZSM-5 (Si/Al = 66), H-Beta (Si/Al = 67) and Del-Al-MCM-22 (Si/Al = 62) catalysts. Reaction conditions: temp., 923 K, others see Fig. 4.

Fig. 12 Changes in selectivities to $C_3^=$ (A), $C_2^=$ (B), $C_4^=$ (C) and BTX (D) with n-hexane conversion on H-ZSM-5 (Si/Al = 66), H-Beta (Si/Al = 67) and Del-Al-MCM-22 (Si/Al = 62) catalysts. Reaction conditions: see Fig. 5.

Fig. 13 IR spectra of H-MCM-22 catalysts with Si/Al ratio of 19 (a), 34 (b), 66 (c) and 100 (d) before (A) and after (B) pyridine was absorbed and desorbed at 423 K for 1 h.

Fig. 14 IR spectra of H-MCM-22 (Si/Al = 19) (a) and Del-Al-MCM-22 catalysts with Si/Al ratio of 39 (b), 56 (c) and 62 (d) before (A) and after (B) pyridine was absorbed and desorbed at 423 K for 1 h.

Fig. 15 IR spectra in the pyridine vibration region of H-MCM-22 (Si/Al = 19) (A) Post-H-MCM-22 (Si/Al = 66) (B) and Del-Al-MCM-22 (Si/Al = 62) (C) catalysts after pyridine adsorption and desorption at 423 K (a), 523 K (b), 623 K (c), and 723 K (d) for 1 h, respectively.

Table 1 Physicochemical properties of various catalysts

| Cat. | $C_{AHFS}$/ M | Si/Al[a] | Al content[b] /mmol $g^{-1}$ | Acid content[c] /mmol $g^{-1}$ | $S_{BET}$[d]/ $m^2$ $g^{-1}$ | $S_{Ext}$[e]/ $m^2$ $g^{-1}$ | $V_{micro}$[e]/ $cm^3$ $g^{-1}$ |
|---|---|---|---|---|---|---|---|
| H-MCM-22 (19) | - | 19 | 0.84 | 0.53 | 517 | 92 | 0.17 |
| H-MCM-22 (34) | - | 34 | 0.48 | 0.37 | 412 | 74 | 0.14 |
| Post-H-MCM-22 (66) | - | 66 | 0.25 | 0.17 | 594 | 96 | 0.20 |
| Post-H-MCM-22 (100) | - | 100 | 0.17 | 0.12 | 562 | 92 | 0.19 |
| Del-Al-MCM-22 (34) | 0.005 | 34 | 0.48 | 0.31 | 497 | 97 | 0.16 |
| Del-Al-MCM-22 (56) | 0.02 | 56 | 0.29 | 0.23 | 466 | 112 | 0.14 |
| Del-Al-MCM-22 (62) | 0.05 | 62 | 0.26 | 0.16 | 450 | 127 | 0.13 |
| H-ZSM-5 (66) | - | 66 | 0.25 | 0.19 | 445 | 24 | 0.18 |
| H-Beta (67) | - | 67 | 0.25 | 0.18 | 587 | 201 | 0.15 |

a Molar ratio determined by ICP.

b Calculated by ICP result.

c Determined by $NH_3$-TPD.

d Measured by $N_2$ adsorption at 77 K.

e Calculated by *t*-plot method.

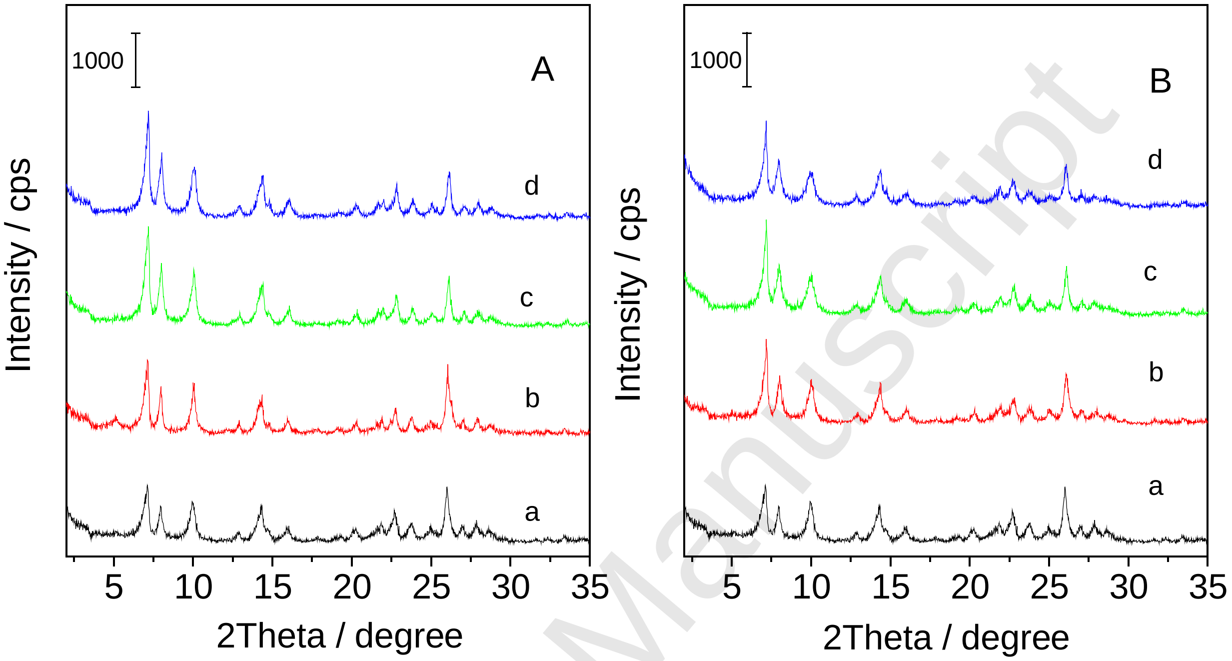

Fig. 1 XRD patterns of H-MCM-22 samples (A) with Si/Al ration of 19 (a), 34 (b), 66 (c) and 100 (d) and Del-Al-MCM-22 samples (B) with Si/Al ratio of 34 (b), 56 (c) and 62 (d).

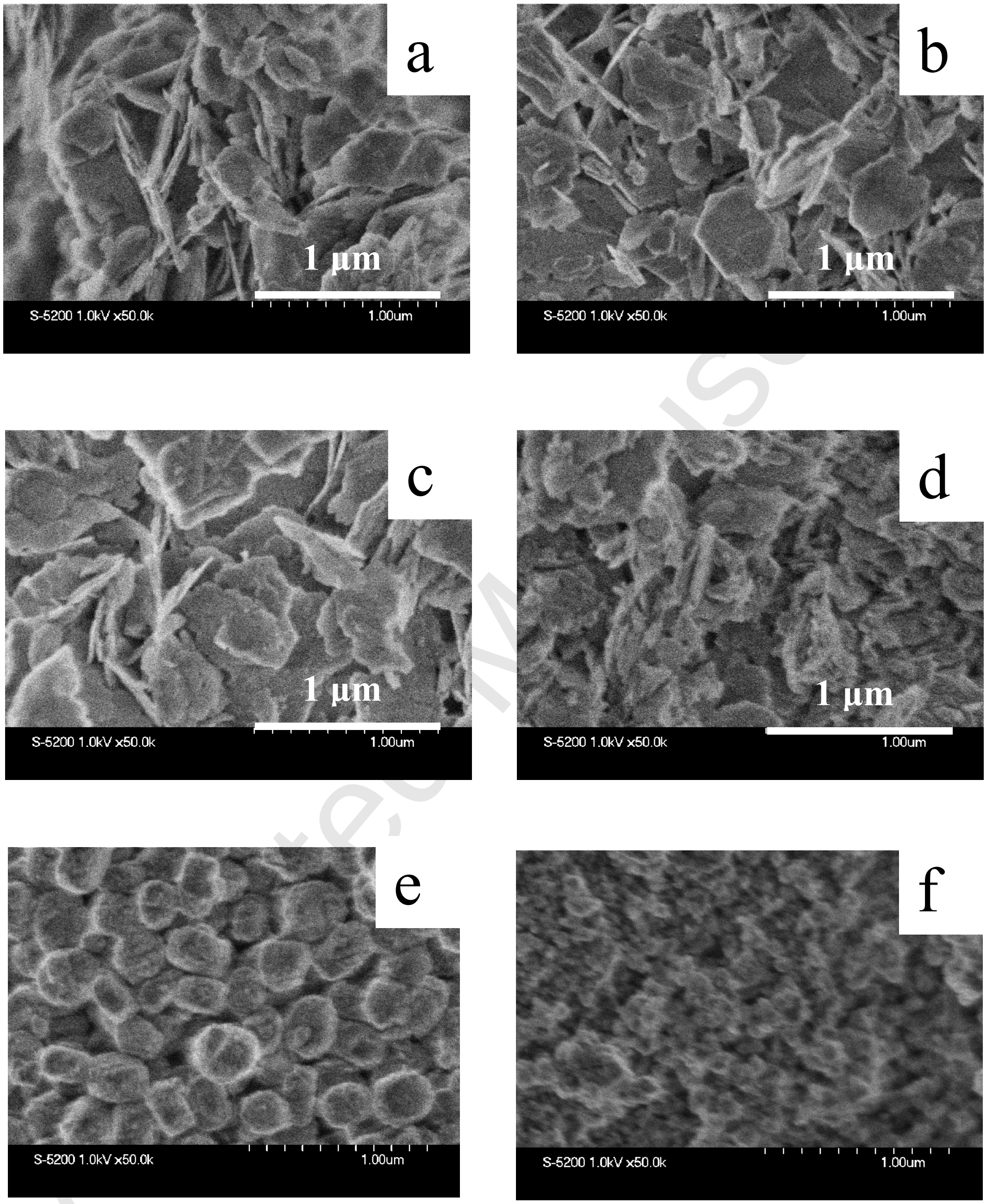

Fig. 2 SEM images of H-MCM-22(Si/Al = 19) (a), Post-H-MCM-22(Si/Al = 100) (b), Del-Al-MCM-22(Si/Al = 34) (c), Del-Al-MCM-22(Si/Al = 62) (d), H-ZSM-5(Si/Al = 66) (e) and H-Beta(Si/Al = 67) (f) samples.

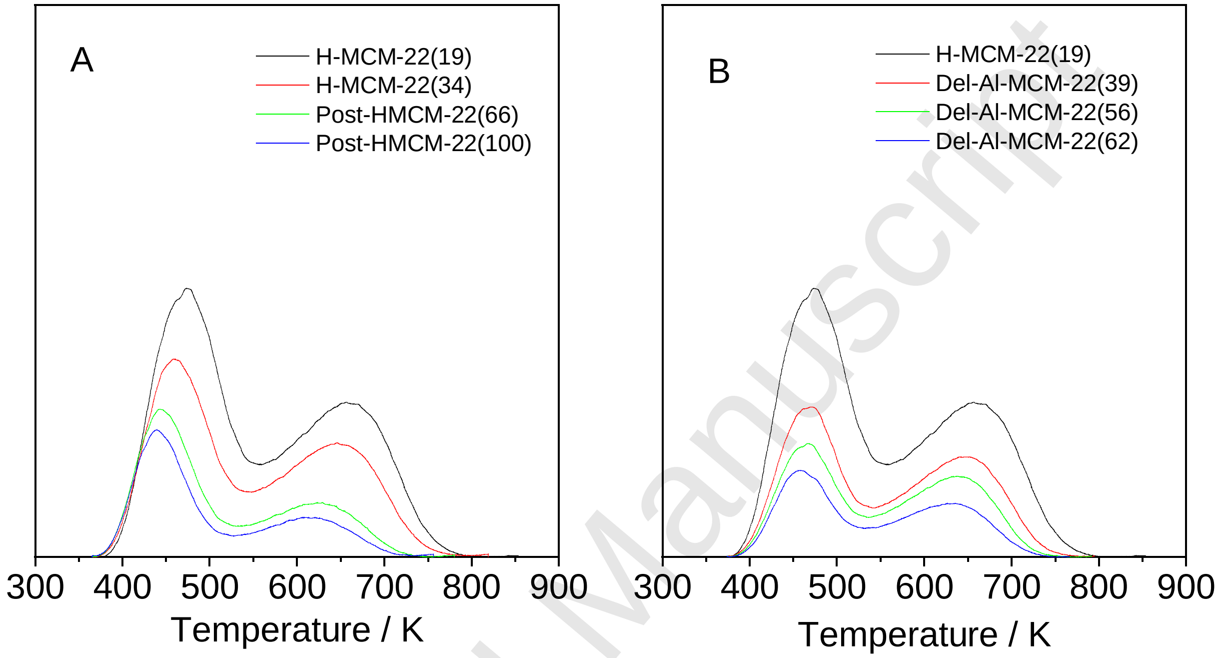

Fig. 3 $NH_3$-TPD profiles of H-MCM-22 (A) and Del-Al-MCM-22 (B) samples with different Si/Al ratios.

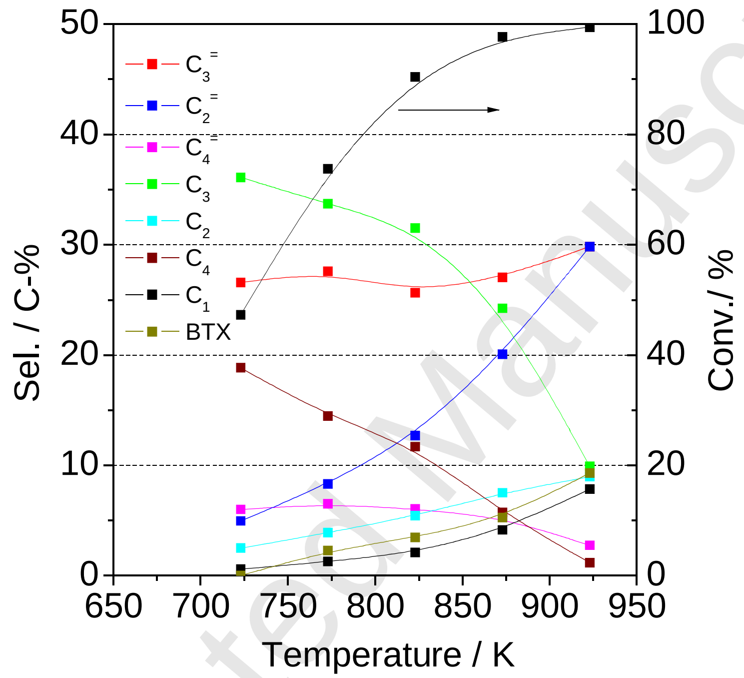

Fig. 4 Effect of reaction temperature on the catalytic cracking of n-hexane on H-MCM-22(Si/Al = 19). Reaction conditions: Cat., 0.1 g; $P_{\text{n-hexane}}$ = 6 kPa; W/F $_{\text{n-hexane}}$ = 64 g-cat h/mol-n-hexane; temp., 723 - 923 K, TOS = 15 min.

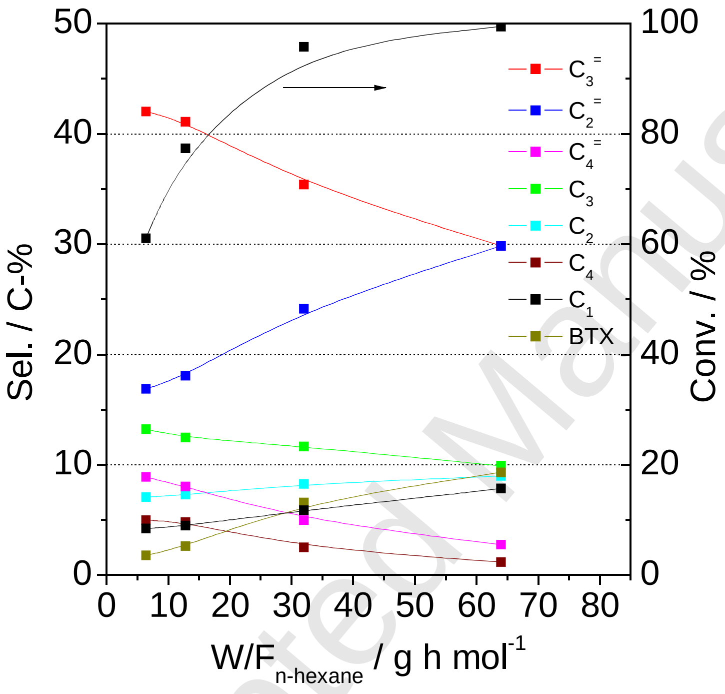

Fig. 5 Effect of contact time on the catalytic cracking of n-hexane on H-MCM-22(Si/Al = 19). Reaction conditions: W/F $_{\text{n-hexane}}$ = 6.4 - 64 g-cat h/mol-n-hexane; temp., 923 K, others see Fig. 4.

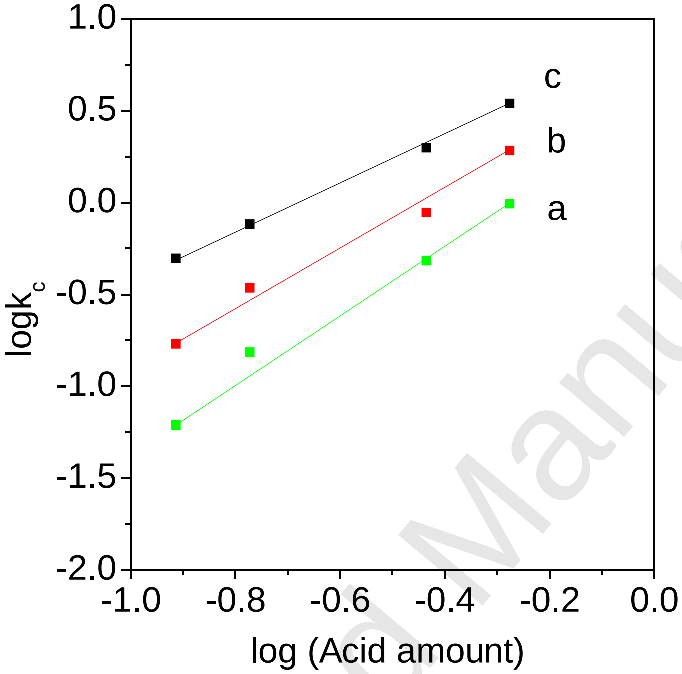

Fig. 6 Dependence of $k_c$ on the acid amount of H-MCM-22 catalysts at different reaction temperatures of 723 K (a), 823 K (b) and 923 K (c).

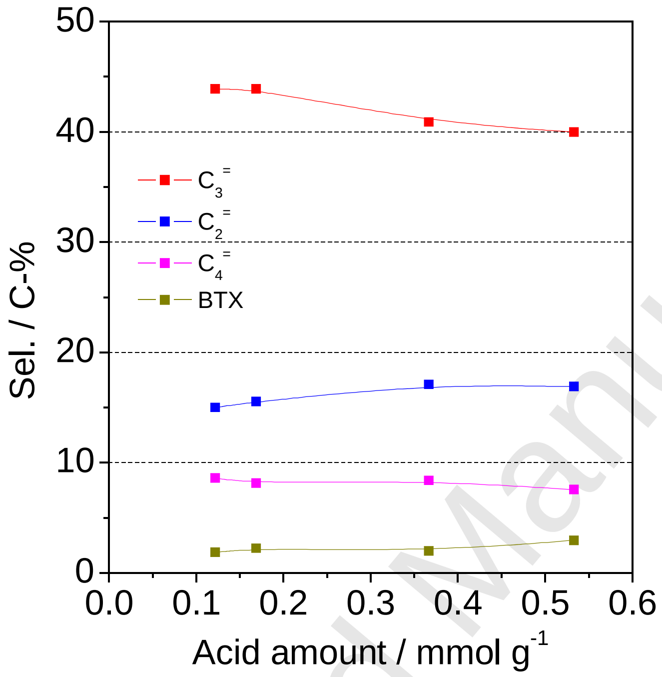

Fig. 7 Relationship between product selectivities and acid amount of H-MCM-22 catalysts at an n-hexane conversion of ca. 80%. Reaction conditions: $P_{\text{n-hexane}}$ = 6 kPa; temp., 923 K, TOS = 15 min.

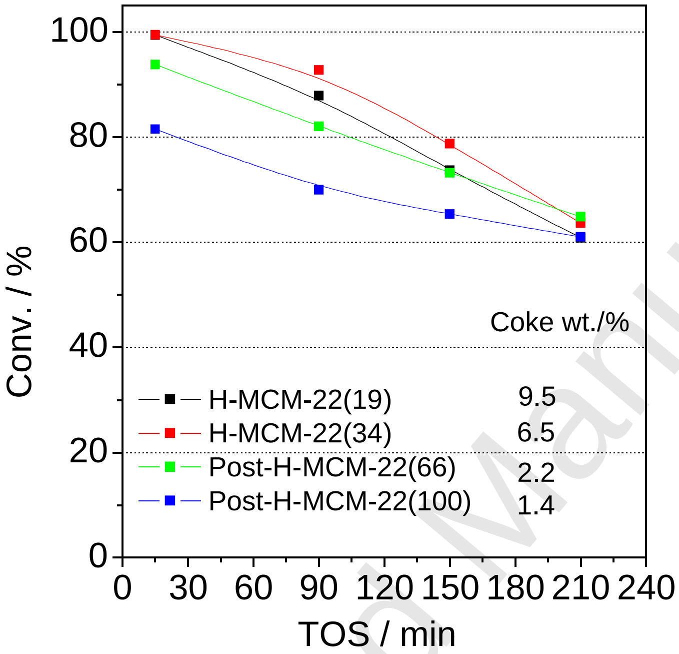

Fig. 8 Change in n-hexane conversion with time on stream (TOS) for H-MCM-22 catalysts with different Si/Al ratios. Reaction conditions: temp., 923 K, others see Fig. 4.

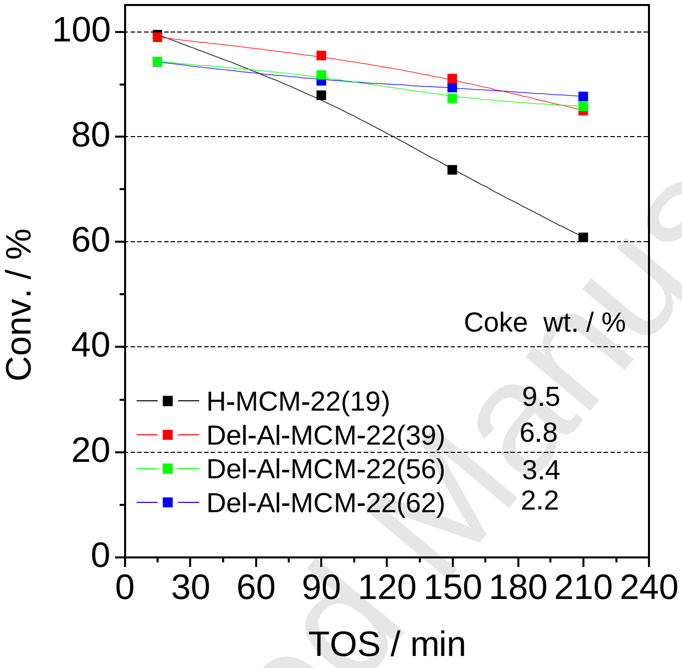

Fig. 9 Change in n-hexane conversion with time on stream (TOS) for H-MCM-22(Si/Al = 19) and Del-Al-MCM-22 catalysts with different Si/Al ratio. Reaction conditions: temp., 923 K, others see Fig. 4.

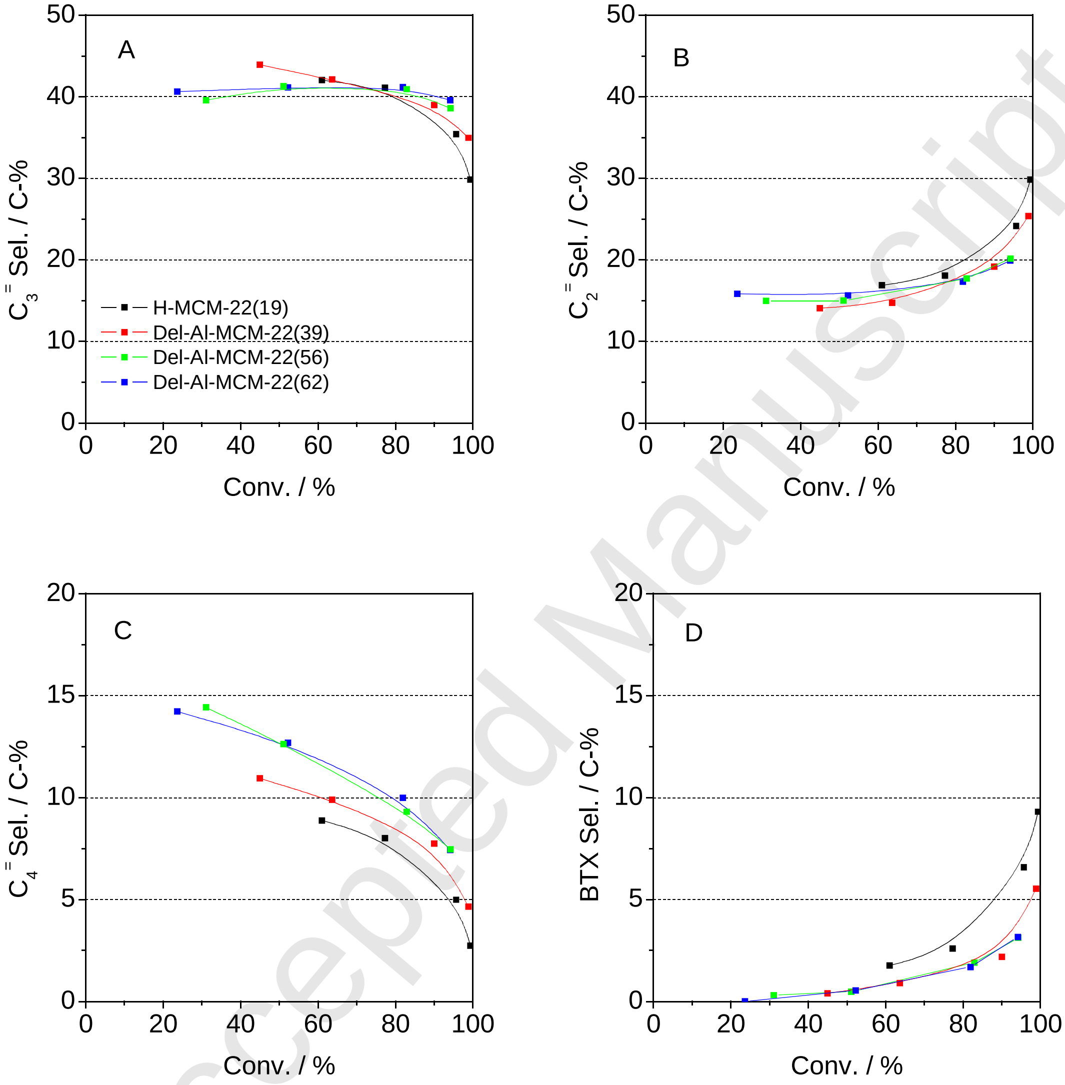

Fig. 10 Changes in selectivities to $C_3^=$ (A), $C_2^=$ (B), $C_4^=$ (C) and BTX (D) with n-hexane conversion on H-MCM-22(Si/Al = 19) and Del-Al-MCM-22 catalysts with different Si/Al ratios. Reaction conditions: see Fig. 5.

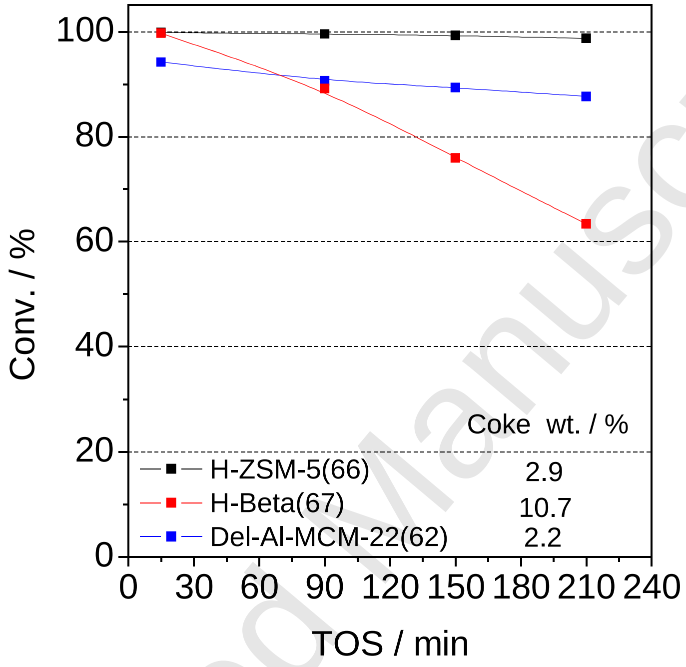

Fig. 11 Change in n-hexane conversion with time on stream (TOS) for H-ZSM-5 (Si/Al = 66), H-Beta (Si/Al = 67) and Del-Al-MCM-22 (Si/Al = 62) catalysts. Reaction conditions: temp., 923 K, others see Fig. 4.

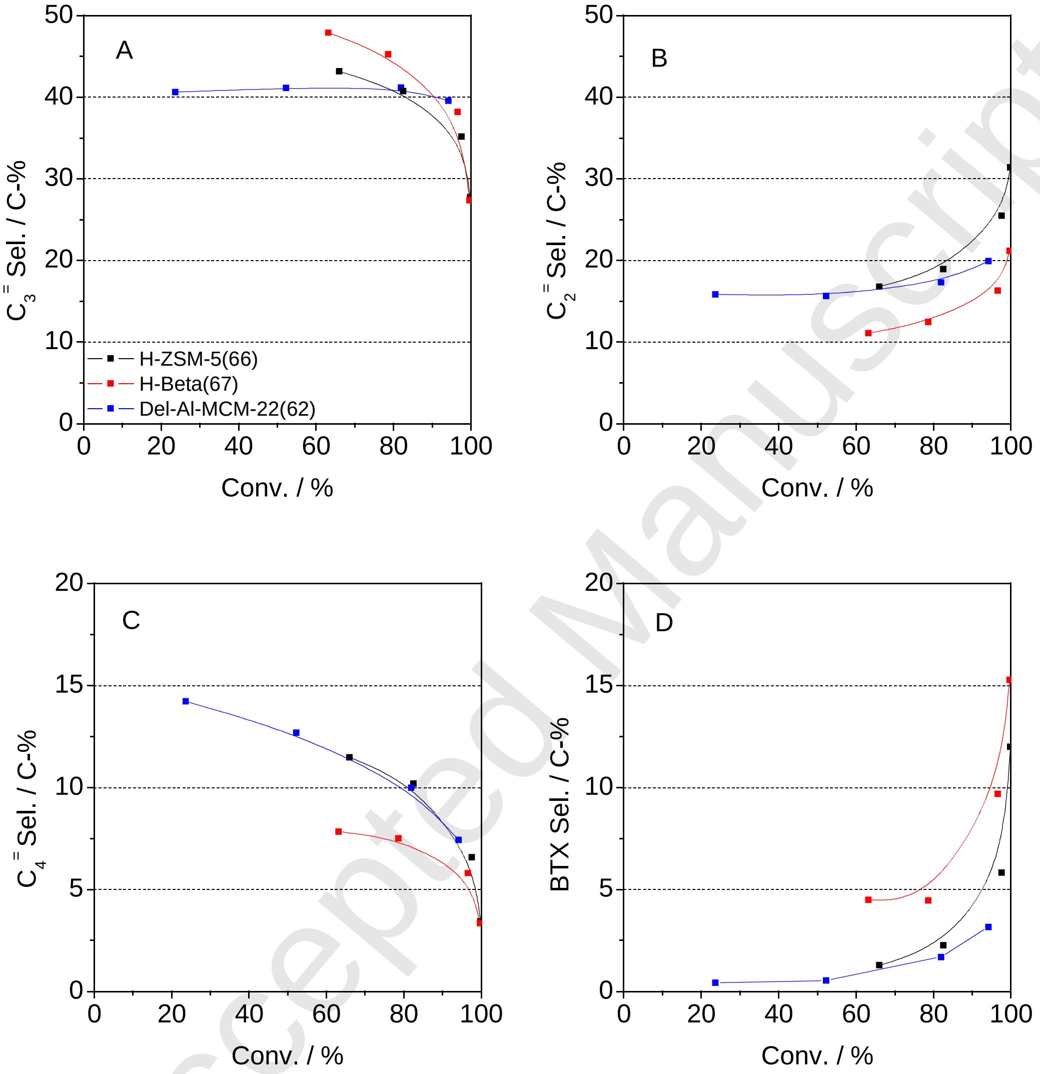

Fig. 12 Changes in selectivities to $C_3^=$ (A), $C_2^=$ (B), $C_4^=$ (C) and BTX (D) with n-hexane conversion on H-ZSM-5 (Si/Al = 66), H-Beta (Si/Al = 67) and Del-Al-MCM-22 (Si/Al = 62) catalysts. Reaction conditions: see Fig. 5.

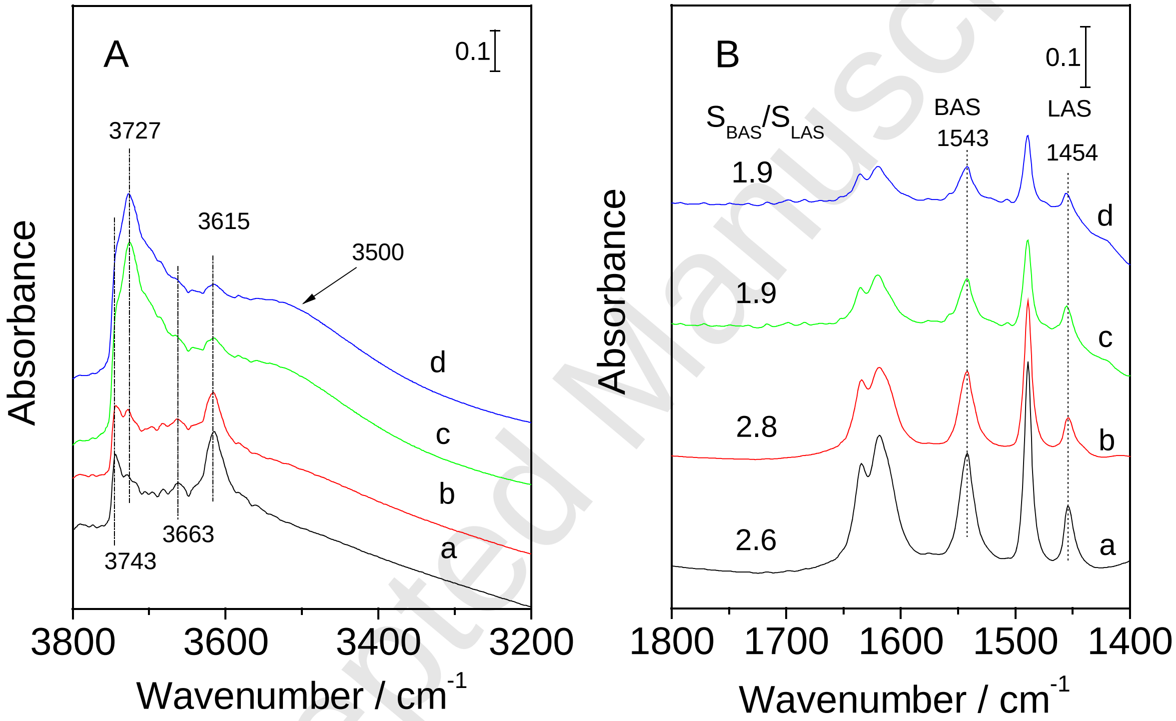

Fig. 13 IR spectra of H-MCM-22 catalysts with Si/Al ratio of 19 (a), 34 (b), 66 (c) and 100 (d) before (A) and after (B) pyridine was absorbed and desorbed at 423 K for 1 h.

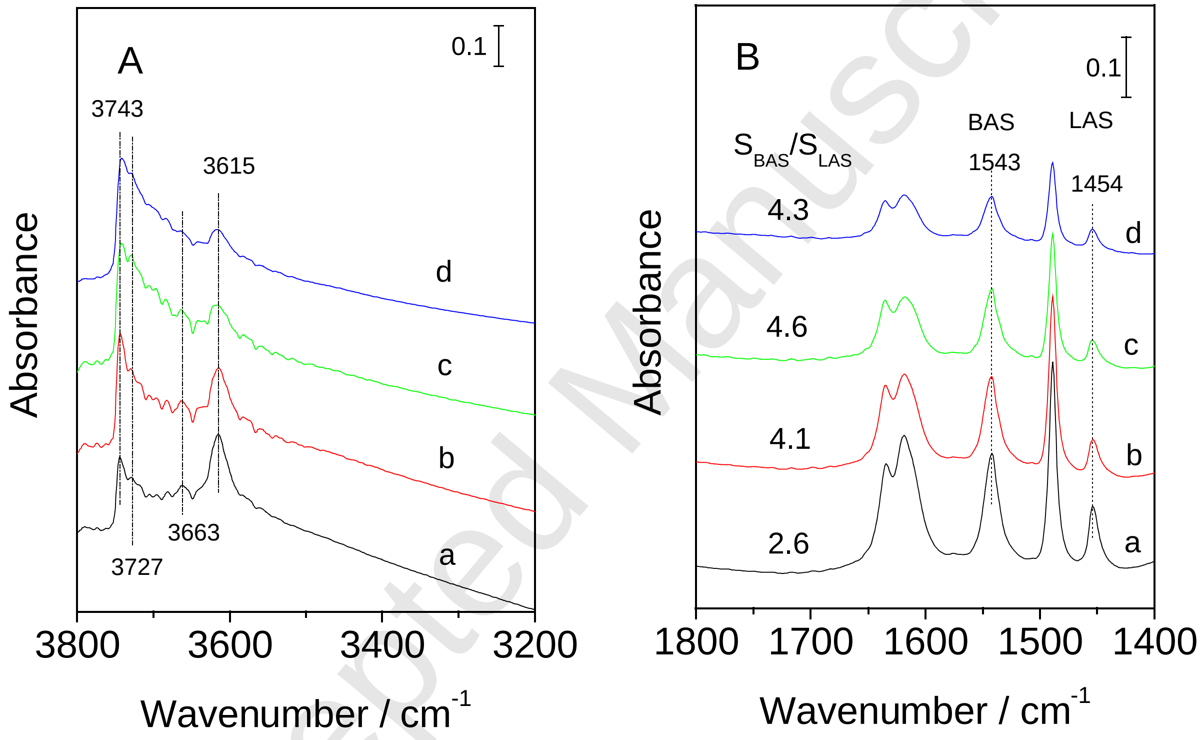

Fig. 14 IR spectra of H-MCM-22 (Si/Al = 19) (a) and Del-Al-MCM-22 catalysts with Si/Al ratio of 39 (b), 56 (c) and 62 (d) before (A) and after (B) pyridine was absorbed and desorbed at 423 K for 1 h.

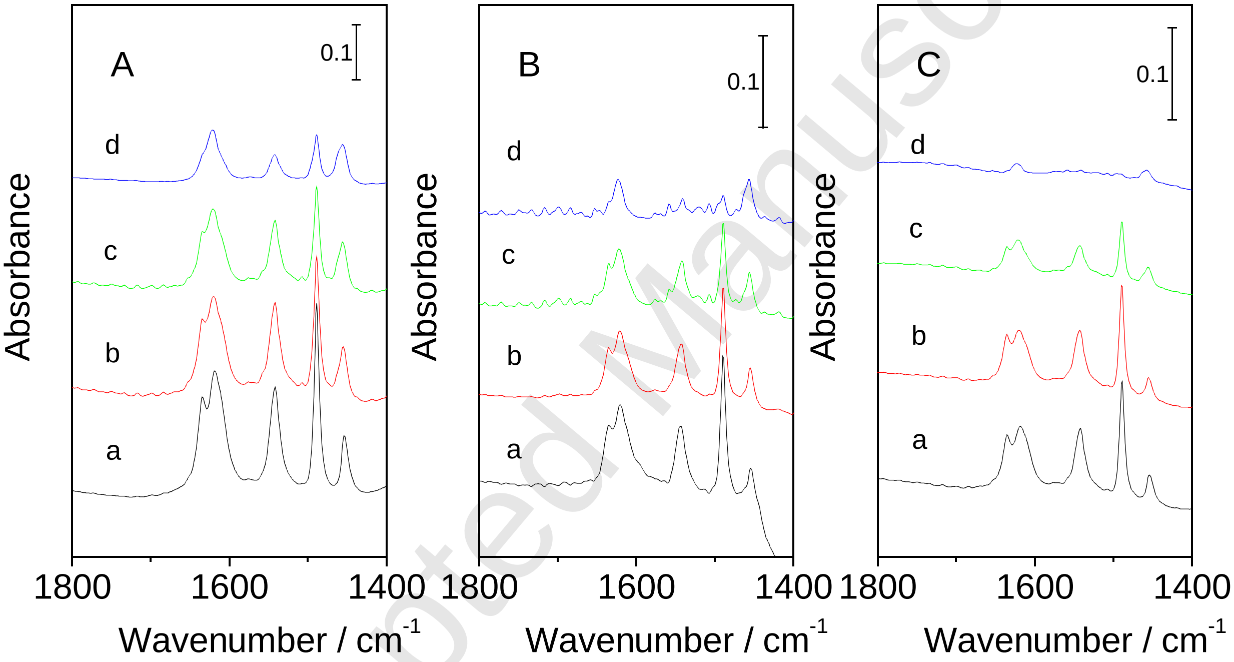

Fig. 15 IR spectra in the pyridine vibration region of H-MCM-22 (Si/Al = 19) (A) Post-H-MCM-22 (Si/Al = 66) (B) and Del-Al-MCM-22 (Si/Al = 62) (C) catalysts after pyridine adsorption and desorption at 423 K (a), 523 K (b), 623 K (c), and 723 K (d) for 1 h, respectively.

# Graphical Abstract

## Catalytic Cracking of n-Hexane for Producing Propylene on MCM-22 Catalysts

Yong Wang, Toshiyuki Yokoi, Seitaro Namba, Junko N. Kondo, Takashi Tatsumi*

*Chemical Resources Laboratory, Tokyo Institute of Technology, 4259 Nagatsuta, Midori-ku, Yokohama 226-8503, Japan*

**E-mail ttatsumi@cat.res.titech.ac.jp (T. Tatsumi), Fax +81 45 924 5282*

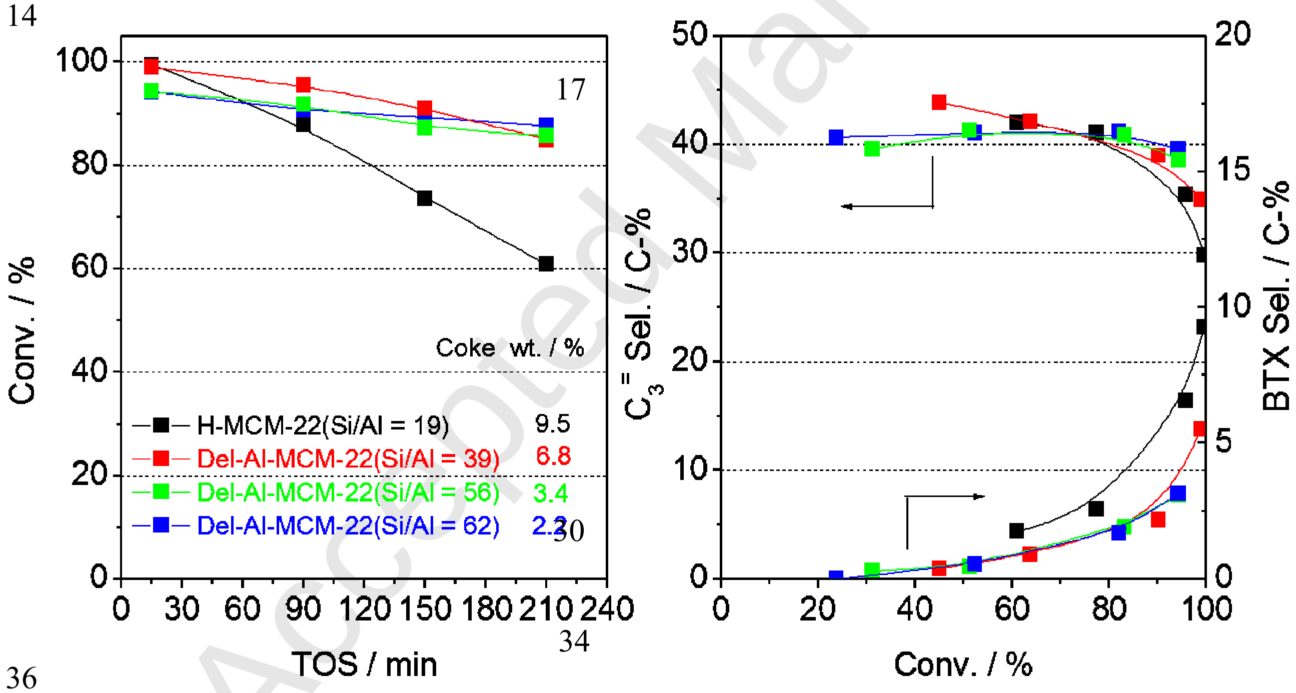

# Highlights

## Catalytic Cracking of n-Hexane for Producing Propylene on MCM-22 Zeolites

Yong Wang, Toshiyuki Yokoi, Seitaro Namba, Junko N. Kondo, Takashi Tatsumi*

*Chemical Resources Laboratory, Tokyo Institute of Technology, 4259 Nagatsuta, Midori-ku, Yokohama 226-8503, Japan*

**E-mail ttatsumi@cat.res.titech.ac.jp (T. Tatsumi), Fax +81 45 924 5282*

- The catalytic performance of MCM-22 zeolites in n-hexane cracking has been investigated at high n-hexane conversions.
- The relationship between the catalytic performance and the acid properties has been investigated.
- MCM-22 zeolites with higher Si/Al ratios exhibited better catalytic performance due to the lower amount and strength of acid sites.
- Dealuminated MCM-22 zeolites by using ammonium hexaflurosilicate (AHFS) treatment showed the higher catalytic life and propylene selectivity at very high n-hexane conversions, due to the smaller amount of Lewis acid sites.